JOC Article

The Unusual Reaction of Semiquinone Radicals with Molecular Oxygen

Luca Valgimigli,*,[#] Riccardo Amorati,[#] Maria Grazia Fumo,[#] Gino A. DiLabio,[†] Gian Franco Pedulli,[#] Keith U. Ingold,[§] and Derek A. Pratt*,[‡]

Dipartimento di Chimica Organica "A. Mangini" via San Giacomo 11, Università di Bologna, 40126 Bologna, Italy, National Institute for Nanotechnology, National Research Council of Canada, 11421 Saskatchewan Drive, Edmonton, AB, Canada T6G 2M9, National Research Council of Canada, 100 Sussex Drive, Ottawa, ON, Canada K1A 0R6, and Department of Chemistry, Queen's University, 90 Bader Lane, Kingston, ON, Canada K7L 3N6

luca.valgimigli@unibo.it; pratt@chem.queensu.ca

Received November 16, 2007

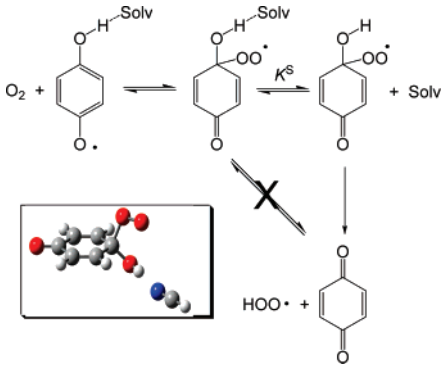

Hydroquinones (benzene-1,4-diols) are naturally occurring chain-breaking antioxidants, whose reactions with peroxyl radicals yield 1,4-semiquinone radicals. Unlike the 1,2-semiquinone radicals derived from catechols (benzene-1,2-diols), the 1,4-semiquinone radicals do not always trap another peroxyl radical, and instead the stoichiometric factor of hydroquinones varies widely between 0 and 2 as a function of ring-substitution and reaction conditions. This variable antioxidant behavior has been attributed to the competing reaction of the 1,4-semiquinone radical with molecular oxygen. Herein we report the results of experiments and theoretical calculations focused on understanding this key reaction. Our experiments, which include detailed kinetic and mechanistic investigations by laser flash photolysis and inhibited autoxidation studies, and our theoretical calculations, which include detailed studies of the reactions of both 1,4-semiquinones and 1,2-semiquinones with O_2, provide many important insights. They show that the reaction of O_2 with 2,5-di-*tert*-butyl-1,4-semiquinone radical (used as model compound) has a rate constant of $2.4 \pm 0.9 \times 10^5$ M^{-1} s^{-1} in acetonitrile and as high as $2.0 \pm 0.9 \times 10^6$ M^{-1} s^{-1} in chlorobenzene, i.e., similar to that previously reported in water at pH ~7. These results, considered alongside our theoretical calculations, suggest that the reaction occurs by an unusual hydrogen atom abstraction mechanism, taking place in a two-step process consisting first of addition of O_2 to the semiquinone radical and second an intramolecular H-atom transfer concerted with elimination of hydroperoxyl to yield the quinone. This reaction appears to be much more facile for 1,4-semiquinones than for their 1,2-isomers.

Introduction

Hydroquinones (benzene-1,4-diols, **I**) are naturally occurring compounds, several of which have been isolated from fungi,[1] algae,[2] and sponges,[3,4] but which are most widely found in plants.[5−9] Many such compounds are known or believed to be

[#] Università di Bologna.
[†] National Institute for Nanotechnology, National Research Council of Canada.
[§] National Research Council of Canada.
[‡] Queen's University.

(1) Abdel-Lateff, A. A.; König, G. M.; Fish, K. M.; Höller, U.; Jones, P. G.; Wright, A. D. *J. Nat. Prod.* **2002**, *65*, 1605−1611.
(2) Aknin, M.; Dayan, T. L.-A.; Rudi, A.; Kashman, Y.; Gaydou, E. M. *J. Agric. Food Chem.* **1999**, *47*, 4175−4177.
(3) Tziveleka, L.-A.; Abatis, D.; Paulus, K.; Bauer, R.; Vagias, C.; Roussis, V. *Chem. Biodiversity* **2005**, *2*, 901−909.

10.1021/jo7024543 CCC: $40.75
Published on Web 02/09/2008

CHART 1

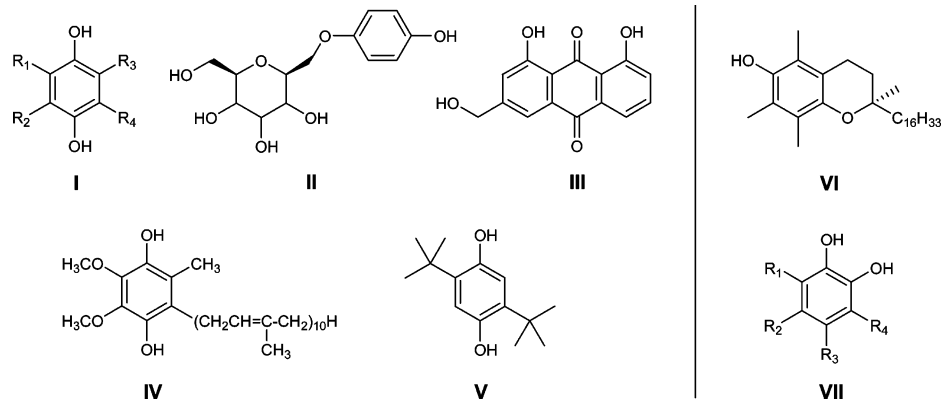

formed when precursors are either hydrolyzed (e.g., **II**, arbutin from *Glycyrrhiza glabra*) or reduced (e.g., **III**, aloe-emodin from *Aloe vera*) in vivo. Most of these natural products have biological activity,[10−16] particularly as anti-inflammatory agents,[17] and several are believed to serve preventive roles against cardiovascular disease, cancer, and other degenerative conditions. Both the anti-inflammatory and preventive actions of hydroquinones are generally ascribed to their radical-trapping chain-breaking antioxidant activities. Ubiquinol (reduced coenzyme Q_{10}, **IV**) is one of the most well-recognized natural product hydroquinones and is believed to be one of the most potent natural chain-breaking antioxidants. Indeed, simple hydroquinones of synthetic origin (e.g., **V**, 2,5-di-*tert*-butyl hydroquinone) are routinely used in industrial applications as antioxidants and have been shown to undergo very fast reaction with peroxyl radicals—the main chain propagating species in lipid peroxidation—with rate constants (k_{inh}) ranging form 3×10^5 to 2×10^6 M^{-1} s^{-1}.[18−20]

Despite their high reactivity toward peroxyl radicals, the role of hydroquinones as chain-breaking antioxidants remains unclear since many of the compounds that have been studied in detail have been found to possess low stoichiometric factors.[18,19] The so-called stoichiometric factor is the number of peroxyl radicals (or peroxidation chain reactions) trapped per molecule of antioxidant. For most phenolic antioxidants, such as α-tocopherol (α-TOH, **VI**), a value of 2 is commonly observed: the first chain-carrying peroxyl radical being trapped by H-atom transfer from the labile phenolic O−H (eq 1) and the second by reaction with the resultant phenoxyl radical (eq 2)

$$ArO{-}H + ROO^{\bullet} \rightarrow ArO^{\bullet} + ROOH \quad (1)$$

$$ArO^{\bullet} + ROO^{\bullet} \rightarrow \text{nonradical products} \quad (2)$$

In autoxidations inhibited by hydroquinones, stoichiometric factors as low as 0.3 have been observed and these values have been shown to be strongly dependent on experimental conditions. This complex behavior clearly differentiates hydroquinones from the isomeric catechols (benzene-1,2-diols; **VII**) that have similar rate constants but are able to trap two peroxyl radicals under most conditions (Scheme 1).[21] The origin of the different stoichiometric factors of the two isomers is unclear.

SCHEME 1

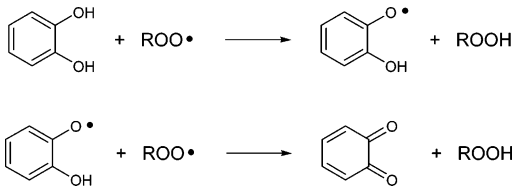

The lower stoichiometric factors observed for hydroquinones and the dependence of these values on experimental conditions have been explained through a chain transfer reaction, wherein a peroxyl radical is quenched by the hydroquinone, but the resultant semiquinone radical reacts with O_2 to generate hydroperoxyl, which can carry on an oxidation chain (Scheme 2). As a result, no net oxidation chains are broken and the stoichiometric factor is zero. The actual stoichiometric factor would then depend on the competition between the reaction of the semiquinone radical with O_2 and its reaction with a peroxyl radical, the kinetics of which may depend on experimental conditions, such as the solvent and the rate of initiation (steady-state concentration of peroxyl radicals).

(4) Shen, Y.-C.; Chen, C.-Y.; Kuo, Y.-H. *J. Nat. Prod.* **2001**, *64*, 801−803.
(5) Parejo, I.; Viladomat, F.; Bastida, J.; Codina, C. *Phytochem. Anal.* **2001**, *12*, 336−339.
(6) Schieber, A.; Keller, P.; Carle, R. *J. Chromatogr., A* **2001**, *910*, 265−273.
(7) Marais, J. P. J.; Mueller-Harvey, I.; Brandt, E. V.; Ferreira, D. *J. Agric. Food Chem.* **2000**, *48*, 3440−3447.
(8) Friedrich, H. *D. Pharm.* **1957**, *12*, 831−834.
(9) Vanhaelen, M.; Vanhaelen-Fastre, R. *J. Chromatogr.* **1983**, *281*, 263−271.
(10) Yang, Y.; Wang, H.; Guo, L.; Chen, Y. *Biomed. Chromatogr.* **2004**, *18*, 112−116.
(11) Yagi, A.; Kabash, A.; Okamura, N.; Haraguchi, H.; Moustafa, S. M.; Khalifa, T. I. *Planta Med.* **2002**, *68*, 957−960.
(12) Rios, J. L.; Bas, E.; Recio, M. C. *Curr. Med. Chem.* **2005**, *4*, 65−80.
(13) Iwai, K.; Kishimoto, N.; Kakino, Y.; Mochida, K.; Fujita, T. *J. Agric. Food Chem.* **2004**, *52*, 4893−4898.
(14) O'Donoghue, J. L. *J. Cosmet. Dermatol.* **2006**, *5*, 196−203.
(15) Halder, R. M.; Richards, G. M. *Skin Ther. Lett.* **2004**, *9*, 1−3. Himejima M.; Nihei K.-I.; Kubo I. *Bioorg. Med. Chem.* **2004**, *12*, 921−925.
(16) Pecere, T.; Gazzola, M. V.; Mucignat, C.; Parolin, C.; Dalla Vecchia, F.; Cavaggioni, A.; Basso, G.; Diaspro, A.; Salvato, B.; Carli, M.; Palu, G. *Cancer Res.* **2000**, *60*, 2800−2804.
(17) Vazquez, B.; Avila, G.; Segua, D.; Escalante, B. *J. Ethnopharm.* **1996**, *55*, 69−75.
(18) Barclay, L. R. C.; Vinqvist, M. R.; Mukai, K.; Itoh, S.; Morimoto, H. *J. Org. Chem.* **1993**, *58*, 7416−7420.
(19) Roginsky V. A.; Barsukova, T. K.; Loshadkin, D.; Pliss, E. *Chem. Phys. Lipids* **2003**, *125*, 49−58.
(20) Loshadkin, D.; Roginsky, V. A.; Pliss, E. *Int. J. Chem. Kinet.* **2002**, *34*, 162−171.
(21) Amorati, R.; Ferroni, F.; Lucarini, M.; Pedulli, G. F.; Valgimigli, L. *J. Org. Chem.* **2002**, *67*, 9295−9303.

SCHEME 2

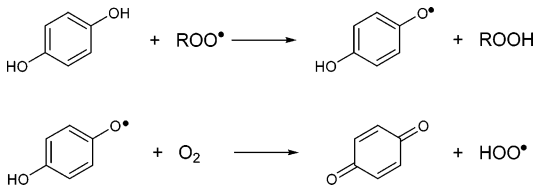

The kinetics and mechanism of the reaction of 1,4-semiquinones with O_2 has been investigated in aqueous media and found to proceed by electron transfer, which becomes particularly facile at neutral to basic pH due to the predominance of the electron-rich semiquinone radical anion (1,4-semiquinone p$K_a \approx 4$).[22−26] Electron transfer to O_2 yields the superoxide radical anion ($O_2^{\bullet-}$), which can be protonated to yield hydroperoxyl (HOO$^\bullet$) and complete the chain transfer at low pH (pK_a of hydroperoxyl is ∼4.8[27]). However, the kinetics and mechanism of such a reaction in aprotic organic media, which is a more appropriate model for lipophilic natural and synthetic hydroquinones such as **IV** and **V**, are hitherto unknown. Moreover, the reason for the different behavior of hydroquinones and catechols is far from clear. To shed some light on these issues, we report here the results of a detailed kinetic and thermodynamic investigation dealing with the fate of the 1,4-semiquinone radical in aerated organic media. The reaction of the semiquinone radical with O_2 has been investigated both by laser flash photolysis (LFP) measurements and by high-level ab initio calculations. Furthermore, the antioxidant activity of 2,5-di-*tert*-butylhydroquinone has been studied by oxygen consumption in the inhibited autoxidation of styrene in different solvents and solvent mixtures, and at different partial pressures of O_2. Kinetic traces have been fit to a kinetic scheme by numerical integration methods to evaluate the exact role of the reaction of the intermediate semiquinone radical with O_2. These results, considered alongside available experimental data and our high-level ab initio calculations on the reaction of 1,2-semiquinone with O_2, clarify the molecular basis for the different behavior of hydroquinones and catechols as radical-trapping chain-breaking antioxidants.

Results and Discussion

I. Laser Flash Photolysis. Nanosecond-pulsed laser flash photolysis of deoxygenated chlorobenzene solutions of 2,5-di-*tert*-butylhydroquinone with or without di-*tert*-butyl peroxide (BOOB) at 308 nm[28] yielded a transient species whose UV−vis spectrum (Figure 1A) was assigned to the corresponding semiquinone radical,[24,26] generated according to the first two reactions of Scheme 3.

When the semiquinone radical was similarly generated in air- or O_2-saturated solutions, the transient absorption maximum at 420 nm decayed as in Figure 1B. On changing the experimental conditions, the lifetime of the semiquinone radical was found to vary with both the O_2 and the initial semiquinone radical concentrations. Simple kinetic analysis of the recorded decay traces was not possible, so we first attempted to reproduce the traces by numerical stochastic simulation, according to the kinetic scheme given by eqs 9−13. We used rate constants available in the literature as initial guesses in these simulations (Table 1) and varied the unknown rate constants, particularly those corresponding to the reaction of the semiquinone with O_2 (see the Supporting Information). The best solutions were then used in iterative numerical fitting of experimental traces using algorithms available as part of Gepasi software (Figure 2).[29] The optimized kinetic constants averaged over several experimental traces obtained in chlorobenzene at 298 K under different experimental conditions (initial concentration of oxygen and semiquinone radical) are reported in Table 1.

To our surprise, the rate constant for the reaction of the semiquinone radical with O_2 in chlorobenzene was quite large (1.3×10^6 M^{-1} s^{-1}) and very close to the value previously reported in water at pH 6.8.[26] While the reaction in water has been shown to occur by electron transfer at neutral or basic pH, either from the semiquinone radical or its deprotonated radical anion, it is difficult to envision it as the mechanism in chlorobenzene. Nevertheless, to further investigate this possibility we repeated experiments under identical conditions using acetonitrile as solvent, a more polar medium ($\epsilon_r = 36$; $E_T(30) = 45.6$ kcal/mol[30]) that would be expected to enhance the rate of electron-transfer reaction as compared to the more apolar chlorobenzene ($\epsilon_r = 5.5$; $E_T(30) = 36.8$ kcal/mol[30]).[28c] Interestingly, upon doing so, the rate constant decreased by an order of magnitude, strongly suggesting that electron transfer is unlikely to be the mechanism of the reaction of semiquinone with O_2.

II. Inhibited Autoxidations of Styrene. Controlled autoxidation of styrene at 303 K initiated by AMVN (or AIBN) and inhibited by 2,5-di-*tert*-butylhydroquinone or by its equally reactive, but more lipid soluble, analogue 2,5-di-*tert*-amylhydroquinone was performed in either chlorobenzene or acetonitrile and oxygen consumption was measured with a differential oxygen uptake apparatus as described previously.[31] The oxygen uptake traces were then subjected to numerical stochastic simulations, using eqs 3−15 as the kinetic model, and subse-

(22) Steenken, S.; Neta, P. *J. Phys. Chem.* **1979**, *83*, 1134−1137.
(23) (a) Roginsky, V. A.; Barsukova, T. K.; Stengmann, H. B. *Chem.-Biol. Interact.* **1999**, *121*, 177−179. (b) Roginsky, V. A.; Pisarenko, L. M.; Bors, W.; Michel, C. *J. Chem. Soc., Perkin Trans. 2* **1999**, 871−876. (c) Roginsky, V. A.; Barsukova, T. K. *J. Chem. Soc., Perkin Trans. 2* **2000**, 1575−1582.
(24) Maisel, D.; Czapski, G. *J. Phys. Chem.* **1975**, *79*, 1503−1509.
(25) Butler, J.; Hoey, B. M.; Swallow, A. J. *FEBS Lett.* **1985**, *182*, 95−98.
(26) Dohrmann, J. K.; Bergmann, B. *J. Phys. Chem.* **1995**, *99*, 1218−1227.
(27) (a) Czapsky, G. *Annu. Rev. Phys. Chem.* **1971**, *22*, 171−208. (b) Bielski, B. H. J.; Cabelli, D. E.; Arudi, R. L.; Ross, A. B. *J. Phys. Chem. Ref. Data* **1985**, *14*, 1041−1100. (c) Christensen, H.; Sehested, K. *J. Phys. Chem.* **1988**, *92*, 3007−3011. (d) Behar, D.; Czapski, G.; Rabani, J.; Dorfman, L. M.; Schwarz, H.A. *J. Phys. Chem.* **1970**, *74*, 3209−3213.
(28) (a) Kazanis, S.; Azarani, A.; Johnston, L. J. *J. Phys. Chem.* **1991**, *95*, 4430−4435. (b) Evans, C.; Scaiano, J. C.; Ingold, K. U. *J. Am. Chem. Soc.* **1992**, *114*, 4589−4593. (c) Valgimigli, L.; Banks, J. T.; Ingold, K. U.; Lusztyk, J. *J. Am. Chem. Soc.* **1995**, *117*, 9966−9971.
(29) (a) Mendes, P. *Comput. Appl. Biosci.* **1993**, *9*, 563−571. (b) Mendes, P. *Trends Biochem. Sci.* **1997**, *22*, 361−363. (c) Mendes, P.; Kell, D. B. *Bioinformatics* **1998**, *14*, 869−883.
(30) Reichardt, C. *Solvents and Solvent Effects in Organic Chemistry*; Verlag Chimie: Weinheim, Germany, 1988.
(31) (a) Lucarini, M.; Pedulli, G. F.; Valgimigli, L.; Amorati R.; Minisci, F. *J. Org. Chem.* **2001**, *66*, 5456−5462. (b) Amorati, R.; Pedulli, G. F.; Valgimigli, L.; Attanasi, O. A.; Filippone, P.; Fiorucci, C.; Saladino, R. *J. Chem. Soc., Perkin Trans. 2* **2001**, 2142−2146.
(32) Rao, P. S.; Hayon E. *J. Phys. Chem.* **1973**, *77*, 2274−2278.
(33) Roginsky, V. A.; Pisarenko, L. M.; Bors, W.; Michel, C.; Saran, M. *J. Chem. Soc., Faraday Trans.* **1998**, *94*, 1835−1840.
(34) Howard, J. A.; Ingold, K. U. *Can. J. Chem.* **1967**, *45*, 785−792.
(35) Foti, M. C.; Ingold, K. U. *J. Agric. Food Chem.* **2003**, *51*, 2758−2765.
(36) Abraham, M. H.; Grellier, P. L.; Prior, D. V.; Morris, J. J.; Taylor, P. J. *J. Chem. Soc., Perkin Trans. 2* **1990**, 521−529.

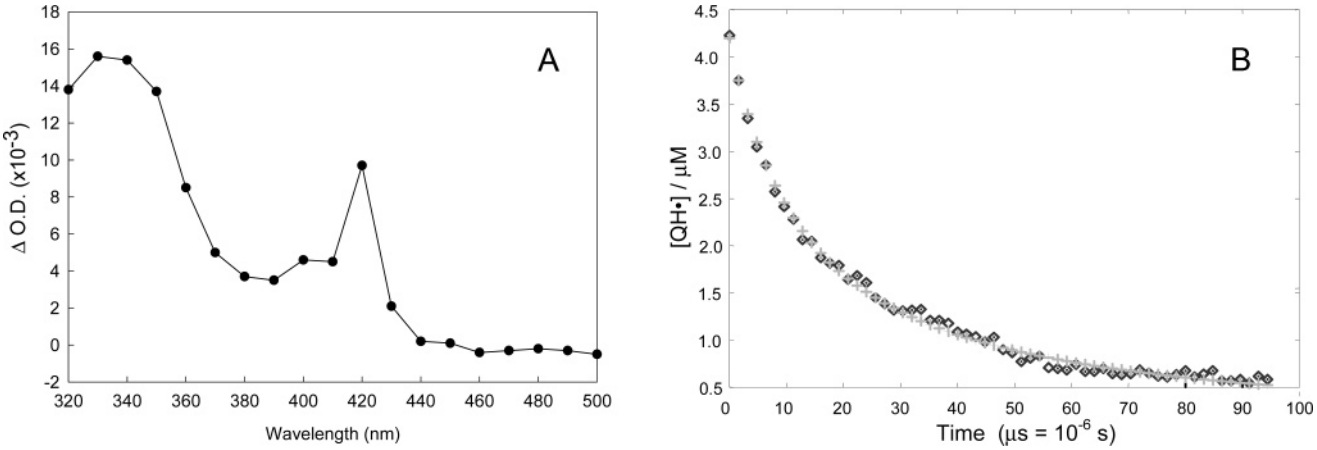

FIGURE 1. (A) UV−vis spectrum of the semiquinone radical 1.4 μs after its generation by laser flash photolysis at 308 nm of a deoxygenated solution of 2,5-di-*tert*-butylhydroquinone (0.2 mM) and di-*tert*-butyl peroxide (4% v/v) in a 0.7 cm sealed quartz cuvette. (B) Decay of the 420 nm transient absorption corresponding to the semiquinone radical in chlorobenzene saturated with oxygen (filled circles) and numerical fitting of the signal trace (crosses) according to the reaction scheme shown in eqs 9−13.

SCHEME 3

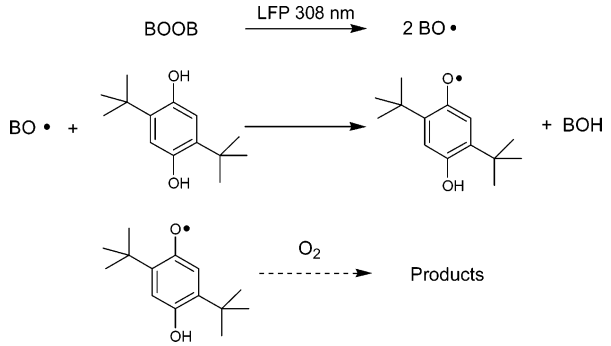

quent fitting/optimization of the best set of kinetic constants with Gepasi software (Figure 2).[21] The results, collected in Table 1, are in excellent agreement with those obtained from the LFP measurements, especially when one considers the difference between the two techniques. Our rate constants are also in satisfying agreement with the few data obtained in organic solvents that are available in the literature. Unfortunately, most of the data reported in previous studies have been obtained in water, and served only as initial values in our simulations. Some representative literature data are listed in Table 1 for comparison.

$$\text{initiator} \rightarrow R^{\bullet} \quad (3)$$

$$R^{\bullet} + O_2 \rightarrow ROO^{\bullet} \quad (4)$$

$$ROO^{\bullet} + RH \rightarrow R^{\bullet} + ROOH \quad (5)$$

$$ROO^{\bullet} + ROO^{\bullet} \rightarrow \text{nonradical products} \quad (6)$$

$$ROO^{\bullet} + QH_2 \rightarrow ROOH + QH^{\bullet} \quad (7)$$

$$QH^{\bullet} + ROO^{\bullet} \rightarrow Q + ROOH \quad (8)$$

$$QH^{\bullet} + QH^{\bullet} \leftrightarrows Q + QH_2 \quad (9)$$

$$QH^{\bullet} + O_2 \leftrightarrows Q + HOO^{\bullet} \quad (10)$$

$$HOO^{\bullet} + QH_2 \leftrightarrows HOOH + QH^{\bullet} \quad (11)$$

$$HOO^{\bullet} + HOO^{\bullet} \rightarrow \text{nonradical products} \quad (12)$$

$$QH^{\bullet} + HOO^{\bullet} \rightarrow \text{nonradical products} \quad (13)$$

$$HOO^{\bullet} + RH \rightarrow H_2O_2 + R^{\bullet} \quad (14)$$

$$HOO^{\bullet} + ROO^{\bullet} \rightarrow \text{nonradical products} \quad (15)$$

To further investigate the kinetic solvent effect on the reaction of the 1,4-semiquinone radical with O_2 and the relevance of this reaction to the antioxidant behavior of hydroquinones, we performed a series of matched styrene autoxidation studies, initiated by 5 mM AMVN at 303 K, using 2,5-di-*tert*-butylhydroquinone (1.0×10^{-5} M) as antioxidant and using solvent mixtures of varying ratios of chlorobenzene/acetonitrile. As is seen in Figure 3, the length of the inhibited period, and hence the stoichiometric coefficient n of the antioxidant, increases dramatically on increasing the amount of acetonitrile in the solvent mixture from 0 ($n = 0.3$) to about 50% ($n = 1.7$). Similar results were obtained with increasing additions of dimethyl sulfoxide (DMSO) as cosolvent in lieu of acetonitrile, although in this latter case a plateau value of n was obtained at a significantly lower concentration of the cosolvent (~0.8 M). Similar sets of experiments were carried out with 2,5-di-*tert*-amylhydroquinone under different conditions (i.e., concentration of the antioxidant and radical initiator, see the Supporting Information) and afforded analogous results.

Similar kinetic solvent effects have been observed in the reactions of phenols with various types of radicals (C-centered, N-centered, and O-centered),[37,40] and have been explained using a model in which hydrogen bond accepting (HBA) solvents "tie-

(37) (a) Avila, D. V.; Ingold, K. U.; Lusztyk, J.; Green, W. H.; Procopio, D. R. *J. Am. Chem. Soc.* **1995**, *117*, 2929−2930. (b) Valgimigli, L.; Ingold, K. U.; Lusztyk, J. *J. Am. Chem. Soc.* **1996**, *118*, 3545−3549. (c) Valgimigli, L.; Banks, J. T.; Lusztyk, J.; Ingold, K. U. *J. Org. Chem.* **1999**, *64*, 3381−3383. (d) Snelgrove, D. W.; Lusztyk, J.; Banks, J. T.; Mulder, P.; Ingold, K. U. *J. Am. Chem. Soc.* **2001**, *123*, 469−477.

(38) Another relevant reaction that causes the decay of the semiquinone radical is the disproportionation of two semiquinone radicals, •QH, to give the quinone (Q) and hydroquinone (QH_2). However, this reaction (eq 9) does not affect the stoichiometric factor with respect to the trapping of a second peroxyl radical by the semiquinone (eq 8), i.e., $n = 2$ (not necessarily as written).

(39) (a) Litwinienko, G.; Ingold, K. U. *J. Org. Chem.* **2003**, *68*, 3433−3438. (b) Litwinienko, G.; Ingold, K. U. *J. Org. Chem.* **2004**, *69*, 5888−5896.

(40) Litwinienko, G.; Ingold, K. U. *Acc. Chem. Res.* **2007**, *40*, 222−230.

TABLE 1. Selected[a] Absolute Rate Constants for Reactions 7 and 9−13 Obtained by Numerical Fitting of the LFP Decay Traces of 2,5-Di-*tert*-butyl-1,4-semiquinone Radical (420 nm) at 298 K and of Oxygen Uptake Traces Recorded During the Azo-Initiated Autoxidation of Styrene Inhibited by 2,5-Di-*tert*-butylhydroquinone at 303 K[i]

	chlorobenzene		acetonitrile		
	LFP	autoxidation	LFP	autoxidation	literature
$k_9/M^{-1}s^{-1}$	$(5 \pm 1) \times 10^9$	5×10^9	$(5 \pm 1) \times 10^9$	5×10^9	1.2×10^9 (water, pH 2.6);[b] 1.3×10^8 (water pH 7.4)[c]
$k_{10}/M^{-1}s^{-1}$	$(1.3 \pm 0.5) \times 10^6$	$(2.4 \pm 0.4) \times 10^6$	$(2.3 \pm 0.7) \times 10^5$	$(2.5 \pm 0.8) \times 10^5$	1.6×10^6 (water)[d]
$k_{-10}/M^{-1}s^{-1}$	$(5 \pm 2) \times 10^9$	5×10^9	$(6 \pm 3) \times 10^8$	6×10^8	$1. \times 10^8$ (water)[d]
$k_{11}/M^{-1}s^{-1}$	$(1.2 \pm 0.8) \times 10^6$	1.6×10^6 [d]	$(1.5 \pm 0.9) \times 10^5$	2.0×10^5 [e]	
$k_{12}/M^{-1}s^{-1}$	1.3×10^9	1.3×10^9	1.0×10^8	1.0×10^8	1.3×10^9 (chlorobenzene);[f] 8×10^7 (acetonitrile, 50 °C)[g]
$k_{13}/M^{-1}s^{-1}$	$(5 \pm 2) \times 10^9$	5×10^9	$(5 \pm 2) \times 10^9$	5×10^9	
$k_7 = k_{inh}/M^{-1}s^{-1}$		$(1.6 \pm 0.4) \times 10^6$		$(2.0 \pm 0.8) \times 10^5$	1.2×10^6 (styrene)[h]

[a] See the Supporting Information for full details. [b] Value for 1,4-quinone from ref 32. [c] Value for 2,5-dimethylhydroquinone from ref 33. [d] Value for 2-*tert*-butylhydroquinone from ref 26. [e] Constrained $k_{11} = k_7$. [f] Data from ref 34. [g] Data from ref 35. [h] Value for 2,5-dimethylhydroquinone from ref 20. [i] Some relevant literature data are reported for comparison. Errors correspond to standard deviation of the optimized kinetic constants on the different experimental traces.

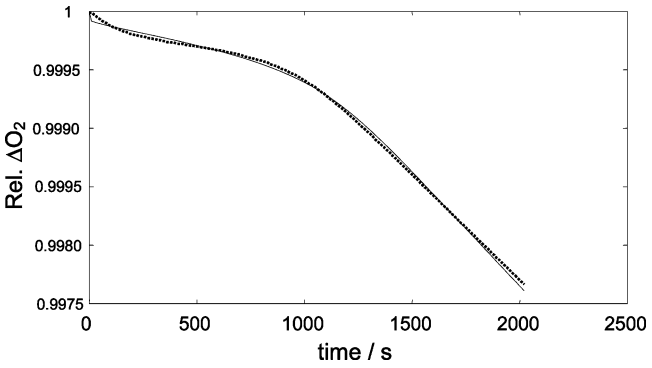

FIGURE 2. Typical oxygen consumption trace recorded during the azo-initiated (AIBN, 303 K) autoxidation of styrene (4.3 M) in chlorobenzene inhibited by 1.25×10^{-5} M 2,5-di-*tert*-amylhydroquinone (dotted line) and its computer simulation using the reaction scheme formed by eqs 3−15 with Gepasi Software (solid line).

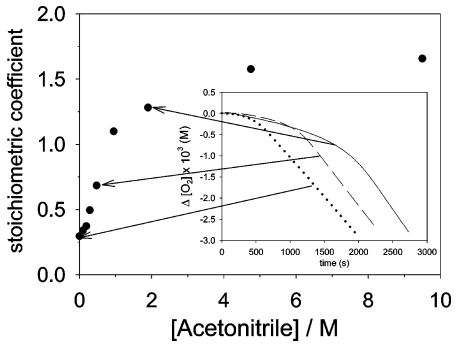

FIGURE 3. Number (n) of peroxyl radicals trapped by each 2,5-di-*tert*-butylhydroquinone (QH_2) molecule (stoichiometric coefficient), obtained by inhibited autoxidation experiments, from the comparison of the QH_2 induction period to that of an equal amount of α-tocopherol ($n = 2$), used as reference antioxidant. Autoxidation conditions: [styrene] = 4.3 M; [QH_2] = 1×10^{-5} M; [AMVN] = 5 mM; [acetonitrile] = 0−9.5 M; in chlorobenzene at 303 K. Insert: Oxygen uptake traces of some representative data points.

up" the labile phenolic H-atom, preventing its abstraction by a radical, and leaving only the non-H-bonded phenol present at equilibrium to react. The observed kinetic solvent effects on the reactions of the semiquinone radical with O_2 can be explained by invoking an analogous model (Scheme 4). In Scheme 4, *S* is a HBA solvent such as acetonitrile ($\beta^H_2 = 0.44$[36]) or DMSO ($\beta^H_2 = 0.78$[36]). For comparison, chlorobenzene is a comparatively weak HBA solvent ($\beta^H_2 = 0.09$[36]). Hydrogen bonding of the O−H moiety in the semiquinone radical to the HBA solvent prevents reaction of the semiquinone with O_2, and its contribution at equilibrium will reduce the overall rate of reaction.[28c,37] The model in Scheme 4 applies only if the reaction proceeds by abstraction of the semiquinone hydrogen atom (direct or stepwise, vide infra) by molecular oxygen, a fascinating reaction that, to the best of our knowledge, has neither been suggested nor studied before.

SCHEME 4

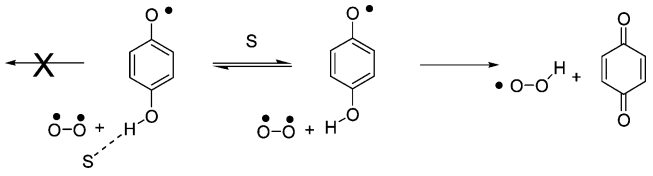

This model also offers an explanation for the change in stoichiometric factor with the change in HBA ability of the solvent (mixture). While the non-H-bonded semiquinone radical can react quantitatively with O_2 (eq 10) leading to a stoichiometric coefficient, $n = 0$, the H-bonded semiquinone radical is unreactive to O_2, but may still react with a peroxyl radical by a non-H-atom transfer mechanism (as do phenoxyls derived from simple phenols) leading to a stoichiometric coefficient, $n = 2$.[38] Since it is possible for the semiquinone radical to interact with the other species present in the reaction mixture (e.g., chlorobenzene, styrene, AIBN, or AMVN, etc.), we have defined a minimum nonzero stoichiometric coefficient c in this model and fit the measured stoichiometric coefficient (n) as a function of the concentration of the HBA cosolvent with eq 16 to obtain

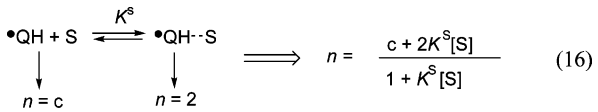

(16)

the equilibrium constant for H-bonding of the semiquinone radical from 2,5-di-*tert*-amylhydroquinone to acetonitrile ($K^S = 1.7 \pm 0.7$ M^{-1}) and DMSO ($K^S = 7.8 \pm 1.4$ M^{-1}). The significance of these equilibrium constants will be discussed later.

III. HAT vs SPLET Mechanism for the Reaction of •QH with O_2. In addition to hydrogen atom transfer (HAT) as the primary mechanism of reaction of phenolic antioxidants with

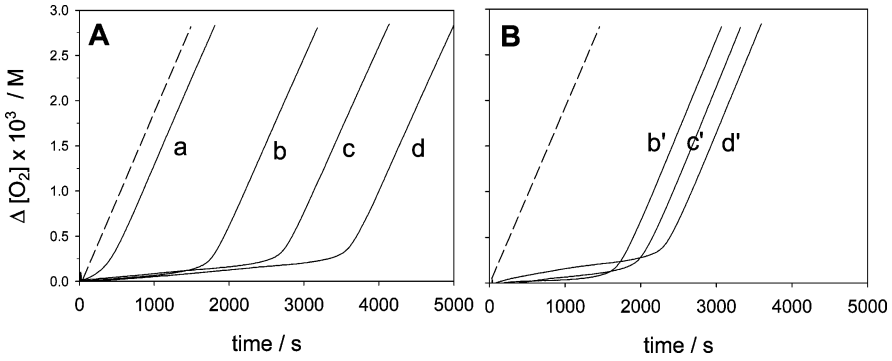

FIGURE 4. Oxygen uptake plots recorded from the inhibited autoxidation of styrene (4.3 M) in chlorobenzene at 303 K, initiated by AMVN (5 mM) in the absence (dashed line) of antioxidants or in the presence (solid lines) of (a) $[QH_2] = 5 \times 10^{-6}$ M, (b) $[\alpha\text{-TOH}] = 5 \times 10^{-6}$ M, (c) a + b, and (d) a + 2b (A) under an atmosphere of air or (B) under an atmosphere of O_2 (b′, c′, d′).

SCHEME 5

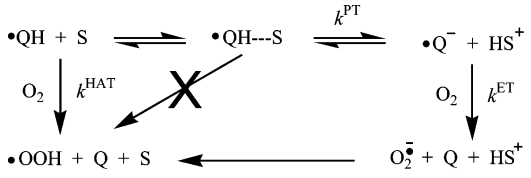

chain-carrying peroxyl radicals and the electron transfer (ET) mechanism sometimes involved in the reaction of very electron-rich phenols with radicals, another mechanism has recently been described: sequential proton loss electron transfer (SPLET),[39−41] which accounts for so-called "anomalous" kinetic solvent effects (unusually fast reactions in polar solvents).

According to the SPLET mechanism, the overall rate of reaction (apparent hydrogen atom transfer) of a phenol with a radical species in a given solvent depends on the small amount of phenoxide present at equilibrium, which is much more reactive than the phenol toward ET. The interplay between these mechanisms, HAT or SPLET, as a function of the experimental conditions has recently been discussed in detail and found to depend on both the electron affinity of the hydrogen accepting reactant and the ability of the solvent to promote phenol ionization.[40] Polar solvents, characterized by high dielectric constants ϵ_r or their ability to solvate anions (as quantified by Swain *A* values[42]), are expected to support the SPLET mechanism.

The reaction of 1,4-semiquinone radicals with O_2 in water ($\epsilon_r = 70$; $A = 1.00$) has been thoroughly investigated and found to proceed via a SPLET-like mechanism (at least at neutral or alkaline pH), i.e., the semiquinone radical anion present at equilibrium undergoes ET to O_2 to form the *p*-quinone and superoxide radical anion. The kinetic solvent effect observed in this investigation suggests that the SPLET mechanism is unlikely to be operating in organic solvents since the rate decreases on going from chlorobenzene ($\epsilon_r = 5.5$; $A = 0.2$) to acetonitrile ($\epsilon_r = 36$; $A = 0.37$) or DMSO ($\epsilon_r = 46.7$; $A = 0.34$). To provide further evidence against the involvement of SPLET in these reactions, we performed matched inhibited styrene autoxidation experiments, in both chlorobenzene and acetonitrile, with or without addition of either 1 mM acetic acid, 1 and 10 mM trichloroacetic acid, or 1 mM *p*-toluenesulfonic acid. In no case did the length of the inhibition period, which determines the magnitude of the stoichiometric factor, change significantly upon addition of the acid.[40]

IV. Autoxidations Inhibited by 2,5-Di-*tert*-butylhydroquinone/α-Tocopherol Co-antioxidant Mixtures. Controlled styrene autoxidation studies (303 K) in chlorobenzene have also been performed with QH_2 as a co-antioxidant along with α-tocopherol (α-TOH). Some of these results are shown in Figure 4A, from which it is clear that α-TOH and QH_2 act synergistically to prolong the inhibition period, similar to previous observations with 4-*tert*-butylcatechol as the co-antioxidant.[21] Under these conditions, peroxyl radicals react partly with QH_2 to form the 1,4-semiquinone radical ($k_{inh} = 1.6 \times 10^6$ M^{-1} s^{-1}) and partly with the more reactive α-TOH to form tocopheroxyl radicals (k_{inh} for α-TOH is 3.2×10^6 M^{-1} s^{-1}, ref 43), from which α-TOH is regenerated by hydrogen atom transfer from QH_2. The fate of the resultant semiquinone radical dictates the efficacy of QH_2 as a co-antioxidant. From the data in Figure 4A, we calculate that the efficiency of tocopherol regeneration by QH_2, α[21] ~0.6, which is significantly lower than the quantitative regeneration ($\alpha = 1$) observed when a catechol (4-*tert*-butylcatechol) is used as a co-antioxidant.[21]

The relevance of the competing reaction of the semiquinone radical with O_2 in determining the co-antioxidant behavior of QH_2 was probed by repeating the autoxidation experiments shown in Figure 4A with a 5-fold increase in the partial pressure of O_2 (Figure 4B). Under these conditions, QH_2 has a negligible effect on the length of the inhibition period, indicating that much of the synergistic behavior of QH_2 with α-TOH is lost.

The importance of oxygen concentration on the fate of the semiquinone radical on the antioxidant (route A) or co-antioxidant (route B) behavior of hydroquinones is illustrated in Scheme 6.

V. Computational Insights on the Mechanism. To help provide some insight into the mechanism of the reaction of O_2 with 1,4-semiquinone radicals and to help understand the differences in antioxidant activity between hydroquinones and catechols, a high-level theoretical study was carried out, the details of which are given in the Method of Calculation section. Two distinct mechanistic possibilities were identified that are consistent with the experimental observations; the first involves a direct H-atom abstraction from the semiquinone by O_2 and

(41) Foti, M. C.; Daquino, C.; Geraci, C. *J. Org. Chem.* **2004**, *69*, 2309−2314.

(42) Swain, C. G.; Swain, M. S.; Powell, A. L.; Alunni, S. *J. Am. Chem. Soc.* **1983**, *105*, 502−523.

(43) Burton, G. W.; Doba, T.; Gabe, E. J.; Hughes, L.; Lee, F. L.; Prasad, L.; Ingold, K. U. *J. Am. Chem. Soc.* **1985**, *107*, 7053−7065.

SCHEME 6

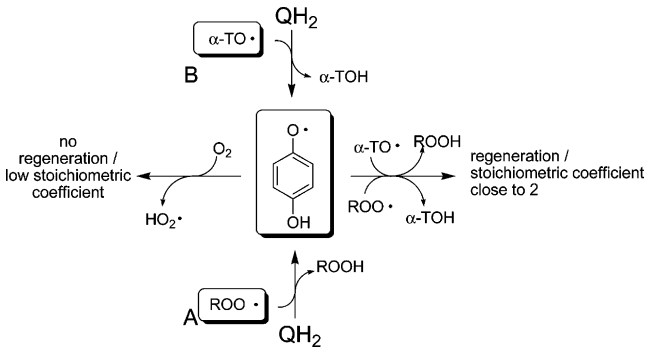

SCHEME 7

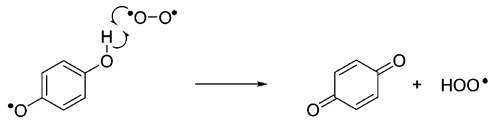

(a) H-Atom Abstraction by O_2

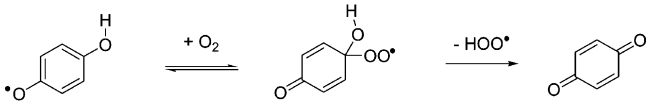

(b) Addition of O_2/Elimination of HOO•

the second involves a two-step reaction: addition of O_2 to the semiquinone followed by elimination of an hydroperoxyl radical (Scheme 7).

(a) H-Atom Abstraction by O_2. H-atom transfer between two oxygen-centered radicals (e.g., aryloxyl and peroxyl such as in the abstraction of a phenolic H-atom by a peroxyl radical, eq 1) is generally a very facile process characterized by low kinetic barriers resulting from favorable orbital interactions in the TS,[44] and being a few kilocalories per mole exothermic for good phenolic antioxidants. In contrast, the abstraction of a phenolic H-atom by molecular oxygen is strongly endothermic (∼30−40 kcal/mol). However, the O−H bond in the hydroperoxyl radical and in the semiquinone radical have roughly the same bond dissociation enthalpies (∼50 kcal/mol) and therefore the abstraction of an H-atom from a semiquinone radical by O_2 is not implausible on thermodynamic grounds. Nevertheless, despite extensive efforts (several different possible trajectories and different guess transition structures generated either manually or with the assistance of the QST2 or QST3 algorithms) no transition structure could be located for H-atom transfer between the 1,4-semiquinone radical and O_2 at various levels of theory. Instead, a stationary point corresponding to an O_2-addition adduct to the carbon bearing the OH group was always found. It was possible to constrain the system to C_s symmetry and obtain a higher order saddle point characterized by a vibrational mode with an imaginary frequency corresponding to the H-atom transfer, but this was one of two such modes for a very high-energy structure. Our inability to locate a transition structure for the concerted transfer of a H-atom between 1,4-semiquinone and O_2 argues against this mechanism.

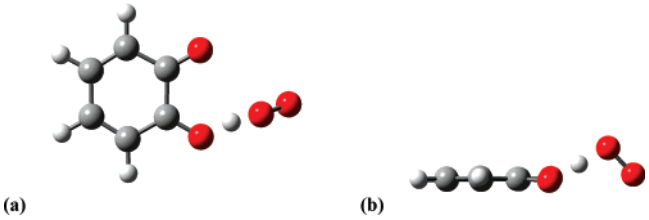

FIGURE 5. Structure of the H-atom transfer transition structure for the reaction of 1,2-semiquinone with O_2 viewed (a) from above the plane of the aromatic ring and (b) in the plane of the aromatic ring.

TABLE 2. Calculated[a] Enthalpies and Free Energies for the Addition of O_2 to 1,4- and 1,2-Semiquinone Radicals

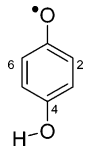

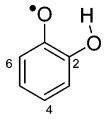

	spin density	ΔH_{298} (kcal/mol)	ΔG_{298} (kcal/mol)	spin density	ΔH_{298} (kcal/mol)	ΔG_{298} (kcal/mol)
2	0.254	2.2	12.2	0.271	4.7	15.2
4	0.311	−3.0	7.4	0.323	−0.2	10.3
6	0.285	4.4	13.9	0.184	5.5	15.6

[a] UCCSD(T)/CBS energies were approximated by using a two-point ROMP2/aug-cc-pV(TZ,DZ) extrapolation of the UCCSD(T)/aug-cc-pVDZ energy at the B3LYP/6-311G(d,p) minimum energy geometries and corrected to enthalpies and free energies at 298 K using the thermochemical corrections calculated at the same level.

In contrast, a transition structure for H-atom transfer between the 1,2-semiquinone radical and O_2 was readily located at various levels of theory and confirmed by vibrational frequency calculations at these levels. The single imaginary mode corresponded to the linear transfer of the H-atom from the semiquinone radical to molecular oxygen ($\angle$(O−H−O) = 170.6°) concomitant with a decreasing and increasing distortion of the semiquinone C−O and C1−C2 bonds, respectively, en route to the *o*-quinone structure. The structure of the TS is shown in Figure 5. The energy of this structure is 25.7 kcal/mol above that of the separated reactants.

(b) Addition of O_2/Elimination of HOO•. This pathway first requires the addition of O_2 to the semiquinone radical to form a peroxyl radical, analogous to the formation of a peroxide from the reaction of O_2 with tri-*tert*-butylphenoxyl radical.[45] Addition of O_2 can, in principle, occur wherever there is unpaired electron spin density in the semiquinone radical. In addition to the phenoxyl oxygen, the unpaired electron density resides on the two ortho and single para carbons. Thus, for both the 1,2-semiquinone and 1,4-semiquinone, we calculated the energy changes for addition of oxygen at each of these positions.[46] The data are shown along with the calculated spin density distributions in Table 2.

A slight preference for addition of O_2 to the para position of both semiquinone radicals would be expected on the basis of

(44) (a) Isborn, C.; Hrovat, D. A.; Borden, W. T.; Mayer, J. M.; Carpenter, B. K. *J. Am. Chem. Soc.* **2005**, *127*, 5794−5795. (b) Zavitsas, A. A. *J. Am. Chem. Soc.* **1972**, *94*, 2779−2789.

(45) Denisov, E. T.; Khudiakov, I. V. *Chem. Rev.* **1987**, *87*, 1313−1357.

(46) These energies could, in principle, be corrected for basis set superposition error (BSSE), which may lead to slightly larger absolute energy barriers and reaction energies for the oxygen addition step. However, given that we are comparing two oxygen addition processes, inclusion of BSSE corrections is unlikely to change the relative energetics. Furthermore, it should be pointed out that there is some concern that BSSE corrections are overestimated in cases where electron correlation is well described, see: Saebø, S.; Tong, W.; Pulay, P. *J. Chem. Phys.* **1993**, *98*, 2170−2175.

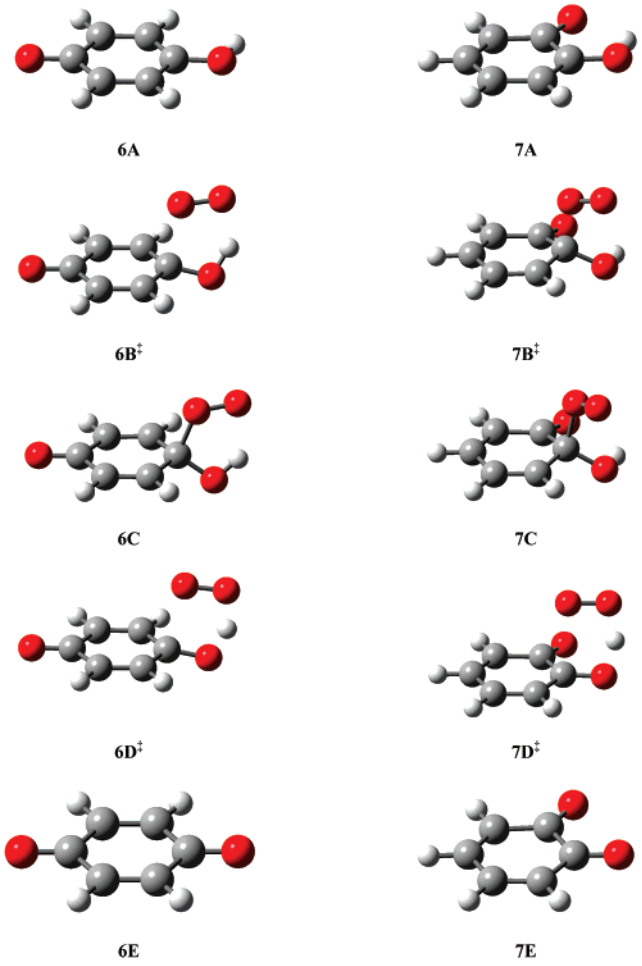

FIGURE 6. Structures of the relevant stationary points characterized along the path for the reaction of the 1,4- and 1,2-semiquinone radicals with O_2.

the calculated spin distributions. Furthermore, addition to the para position would appear to be most favorable on an energetic basis in both cases. For the 1,4-semiquinone, addition to the para position yields a peroxyl radical that is stabilized by the formation of an intramolecular H-bond as well as through hyperconjugation between the σ_{C-OO}* and a lone pair of the oxygen atom of the geminal hydroxyl group (**6C** in Figure 6). Addition to the ortho positions leads to no such stabilization, as the neighboring carbonyl group (formerly the aryloxyl C−O•) inductively withdraws electrons from the C−OO• moiety, destabilizing it. The differences in the energetics between the O_2-adducts of the 1,2-semiquinone are similar; there remains a large preference for the para position. While addition to the ortho carbon, which bears the hydroxyl group (**7C** in Figure 6), can benefit from hyperconjugation, this is somewhat negated by the change in geometry at carbon, which disrupts the intramolecular H-bond as well as the inductively electron-withdrawing effect of the neighboring carbonyl group (formerly the aryloxyl C−O•). However, since this is the O_2 addition adduct that can undergo reaction (vide infra), we show its structure (**7C**) as well as that of the corresponding adduct derived from the 1,4-semiquinone (**6C**) in Figure 6.

Thus, consideration of both the spin distribution and energetics indicates that addition of O_2 to the para position of the 1,4-semiquinone radical is quite facile, and we have found that this adduct readily undergoes a concerted H-atom transfer/elimination reaction to yield the 1,4-quinone and hydroperoxyl radical. Thus, elongation of the C−OO• bond is concerted with transfer of the H-atom from the O−H group to the OO• moiety. The transition structure for this process was calculated to be higher in energy than the O_2 adduct by 5.4 kcal/mol. Similarly, we found a TS for concerted H-atom transfer/elimination from the ortho O_2 adduct of the 1,2-semiquinone radical, which was 8.3 kcal/mol higher in energy than the adduct. The transition state structures are also shown in Figure 6 (**6D**‡ and **7D**‡).

It is of interest to compare the two transition structures **6D**‡ and **7D**‡. A visual inspection of the structures supports an earlier TS for elimination of hydroperoxyl from the O_2 adduct of the 1,4-semiquinone compared to that of the 1,2-semiquinone where a strong intramolecular H-bond must be broken. This is clear from the more planar sp^2-like geometry of the peroxyl-bearing carbon in **7D**‡ compared to the nonplanar sp^3-like geometry of the peroxyl-bearing carbon in **6D**‡. Indeed, the C−OO• bond is longer in **7D**‡ (2.33 Å) compared to **6D**‡ (2.22 Å). Furthermore, the H-atom is closer to the departing dioxygen moiety in the former TS structure (1.24 Å) compared to the latter (1.31 Å).

Figure 7 summarizes the calculated relative enthalpies of the key stationary points that we have characterized for the reaction of the 1,2- and 1,4-semiquinone radicals with O_2 and highlights the factors that distinguish 1,2- and 1,4-hydroquinones as antioxidants. Thus, not only does the 1,4-semiquinone radical undergo a more thermodynamically favorable reaction with O_2 than does the 1,2-semiquinone radical by 7.7 kcal/mol, but this reaction also has a lower enthalpic barrier by 3.0 kcal/mol. Much of this difference is undoubtedly due to disruption of the intramolecular H-bond in the 1,2-semiquinone upon addition of O_2. In the second step, the intramolecular H-bond in the O_2-adduct of the 1,2-semiquinone radical must be completely broken to yield the TS, which is consistent with the larger enthalpic barrier to elimination when compared to the O_2-adduct of the 1,4-semiquinone radical of 3.0 kcal/mol. Accordingly, it would appear that the intramolecular H-bond in the 1,2-semiquinone is a major factor in moderating its reaction with O_2, accounting for why catechols are generally more effective antioxidants or co-antioxidants under most conditions.

Our calculations indicate that the reaction of 1,4-semiquinone radical with O_2 is overall slightly endothermic (because the reaction involves the same number of reactants and products, the entropy factor can be considered negligible, so ΔH is approximately equal to ΔG), which is in agreement both with our kinetic measurements (k_{10}/k_{-10} is $\sim 4 \times 10^{-4}$ in chlorobenzene, see Table 1) and, at least at a qualitative level, with our experimental thermodynamics (vide infra) and previous computational efforts by Wang and Eriksson.[47] At first glance, it would appear that these results contradict a recent theoretical study by Bobrowski et al.,[48] who carried out calculations at various levels of theory including CASSCF and CASSCF/MRMP, and found it exothermic. However, it should be pointed out that their calculated enthalpy was for the reaction of 1,4-semiquinone radical and O_2 to yield a H-bonded 1,4-quinone:hydroperoxyl product complex, which drops the reaction energy in the gas phase to yield an exothermic reaction enthalpy.

(47) Wang, Y.-N.; Eriksson, L. A. *Theor. Chim. Acc.* **2001**, *106*, 158−162.

(48) Bobrowski, M.; Liwo, A.; Hirao, K. *J. Phys. Chem. B* **2007**, *111*, 3543−3549.

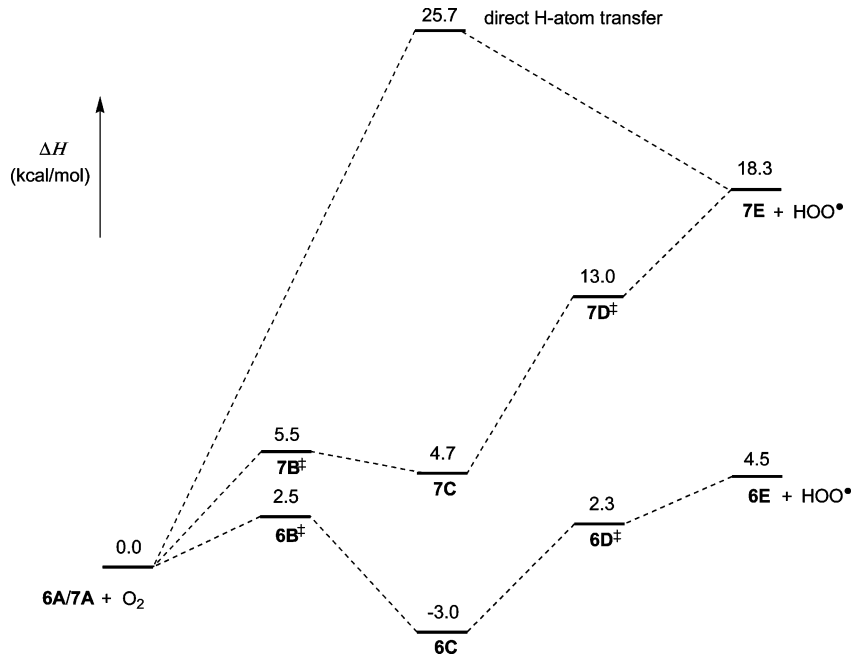

FIGURE 7. Relative enthalpies of the relevant stationary points characterized along the path for the reaction of the 1,2- and 1,4-semiquinone radicals with O_2. UCCSD(T)/CBS energies were approximated using a two-point ROMP2/aug-cc-pV(TZ,DZ) extrapolation of the UCCSD(T)/aug-cc-pVDZ energy at the B3LYP/6-311G(d,p) minimum energy geometries and corrected to enthalpies at 298 K using the thermochemical corrections calculated at the same level. **6A**−**6E** and **7A**−**7E** are shown in Figure 6 (Note: entropic contributions decrease the relative energies of **6E** + HOO• and **7E** + HOO• below those of **6D**‡ and **7D**‡, respectively).

TABLE 3. Comparison of Calculated Activation Energies for Elimination of Hydroperoxyl from Peroxyl Radicals Derived from Methanol, Ethanol, and Isopropanol with Experimental Data[46]

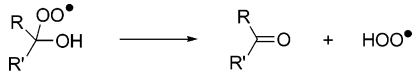

R	R′	exptl k (s^{-1})	exptl E_a (kcal/mol)	calcd E_a (kcal/mol)	exptl $\Delta S^{\ddagger}$ (cal/(mol K))	calcd $\Delta S^{\ddagger}$ (cal/(mol K))
H	H	<10	n/a	11.9	n/a	−4.1
H	Me	52	n/a	11.3	n/a	−1.4
Me	Me	665	13.5	9.9	−3.0	1.0

[a] UCCSD(T)/CBS energies were approximated from the UCCSD(T)/aug-cc-pVDZ energy by using a two-point ROMP2/aug-cc-pV(TZ,DZ) extrapolation scheme at B3LYP/6-311G(d,p) geometries, whose nature as stationary points was confirmed by vibrational frequency calculations at the same level, which provided necessary thermochemical corrections to obtain values of E_a (i.e., $E_a = \Delta H^{\ddagger} + RT$).

There is precedent for the elimination mechanism we have proposed here. Some years ago, Schulte-Frohlinde and co-workers[49] demonstrated by photoflash conductivity measurements in water that peroxyl radicals derived from simple alcohols eliminate hydroperoxyl in a unimolecular, concerted fashion to yield the corresponding carbonyl compounds. The first-order rate constants for these reactions were <10, 52, and 665 s^{-1} for the peroxyls derived from methanol, ethanol, and isopropanol, respectively, and Arrhenius studies on the last yielded $E_a = 13.5$ kcal/mol and $\Delta S^{\ddagger} = -3$ cal/(mol K) (see Table 3).

The observation of increasing rate constants with increasing methyl substitution was explained on the basis of increased stability of the product carbonyl as a function of higher alkyl substitution. The stability of a 1,4-quinone product formed by elimination of hydroperoxyl from the 1,4-semiquinone-derived peroxyl radical may be expected to lead to an even faster reaction rate. Indeed, our calculated E_a for this process is 5.9 kcal/mol (vide supra), whereas that which we calculate for elimination of hydroperoxyl from isopropanol is ca. 9.9 kcal/mol (see Table 3).[50] This difference in E_a of 4.0 kcal/mol corresponds to a 860-fold increase in rate constant (assuming similar A-factors, which is supported by our calculations[51]), and is fully consistent with our measured rate constants and that reported in water at acidic pH.

VI. Experimental Thermodynamics. Theoretical calculations nicely account for the differing reactivity of 1,2- and 1,4-semiquinone radicals with O_2, predicting that H-atom transfer from 1,2-semiquinone radicals to O_2 (direct or stepwise) is overall more energetically demanding than the analogous reaction involving 1,4-semiquinone, with a difference in the two enthalpies of reaction of close to 14 kcal/mol. To check the validity of these predictions it would be useful to have experimental data affording the $\Delta H°$ associated with these reactions. The gas-phase standard enthalpy of formation ($\Delta H°_f$) of the 1,2- and 1,4-quinones have recently been made available by Fattahi et al. as −21.0 and −27.7 kcal/mol, respectively.[52] When combined with the gas-phase standard enthalpy of formation of the HOO• radical ($\Delta H°_f = +3.2$ kcal/mol)[53] these data would afford experimental validation of the calculated data

(49) Bothe, E.; Behrens, G.; Shulte-Frohlinde, D. *Z. Naturforsch. B* **1977**, *32*, 886−889.

(50) When an explicit water molecule is included in the calculation, acting as an H-bond acceptor to the alcohol moiety in the peroxyl radical and the "in-flight" H-atom in the TS, $E_a = 14.8$ kcal/mol, in much better agreement with the experimental value of 13.5 kcal/mol.

(51) Our calculations yield $\Delta S^{\ddagger} = -0.3$ cal/(mol K) for elimination of hydroperoxyl from the O_2 adduct of 1,4-semiquinone.

(52) Fattahi, A.; Kass, S. R.; Liebman, J. F.; Matos, M. A. R.; Miranda, M. S.; Morais, V. M. F. *J. Am. Chem. Soc.* **2005**, *127*, 6116−6122.

(53) Ramond, T. M.; Blanksby, S. J.; Kato, S.; Bierbaum, V. M.; Davico, G. E.; Schwartz, R. L.; Lineberger, W. C.; Ellison, G. B. *J. Phys. Chem. A* **2002**, *106*, 9641−9647.

SCHEME 8

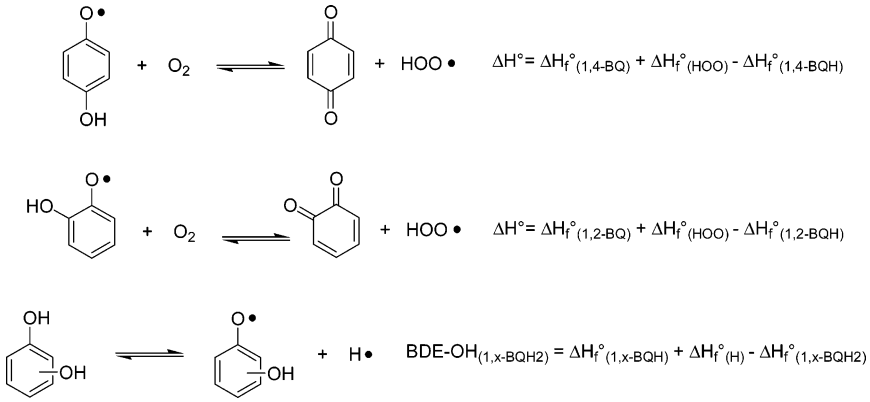

provided the standard enthalpy of formation for the 1,2- and 1,4-semiquinone radicals were also available (Scheme 8).

An accurate measurement of the BDE_{OH} for catechol by the Radical-Equilibration Electron Paramagnetic Resonance (REqEPR) technique has recently been reported by some of us as +81.8 kcal/mol.[54] Measured in isooctane in the absence of photochemical initiators, this provides a reasonable approximation to gas-phase conditions. This value must be decreased by 1.1 kcal/mol because of the revision of the heat of formation of *E*-azobenzene,[55] yielding BDE_{OH}(catechol) = +80.7 kcal/mol. When combined with the available values for the gas-phase standard enthalpy of formation of the hydrogen atom ($\Delta H°_f$ = +52.1 kcal/mol)[56] and catechol (−63.9 kcal/mol)[57] it provides the desired value $\Delta H°_f$(1,2-BQH•) = −35.3 kcal/mol. This yields an enthalpy of reaction between the 1,2-semiquinone radical and O_2 of $\Delta H°_r$ = 17.5 kcal/mol, in good agreement with the calculated value of 18.3 kcal/mol.

Unfortunately no equally reliable value is available for the BDE_{OH} of hydroquinone. To provide one, we measured the BDE_{OH} for 2,5-di-*tert*-amylhydroquinone by the REqEPR technique, by direct photolysis of isooctane solutions containing variable amounts of BHT (revised[55] BDE_{OH} = 79.9 kcal/mol) as reference compound (ArOH). Comparison of the digitized experimental spectra with computer simulated spectra afforded the equilibrium constant for eq 17 from which the BDE_{OH} for 2,5-di-*tert*-amylhydroquinone could be obtained according to eq 18, with the usual assumption that the entropy term can be neglected.[58]

$$\text{di-}t\text{-AmBQH}_2 + \text{ArO}^\bullet \rightleftharpoons \text{di-}t\text{-AmBQH}^\bullet + \text{ArOH} \quad (17)$$

$$\text{BDE(di-}t\text{-Am-1,4-BQH}_2) \cong \text{BDE(ArOH)} - RT\ln(K_e) \quad (18)$$

By correcting the resulting BDE_{OH}(di-*t*-Am-1,4-BQH_2) = 79.2 ± 0.15 kcal/mol for the additive contribution[59] of para (−1.75 kcal/mol) and meta (−0.5 kcal/mol) *tert*-alkyl substituents, the desired value for BDE_{OH} of hydroquinone was obtained as +81.5 kcal/mol.[60] This value can be combined with the available gas-phase standard enthalpy of formation of the hydrogen atom ($\Delta H°_f$ = +52.1 kcal/mol)[53] and hydroquinone ($\Delta H°_f$ = −63.4 kcal/mol)[61] to give the gas-phase standard enthalpy of formation of the 1,4-semiquinone radical, $\Delta H°_f$ = −33.9 kcal/mol. This yields an enthalpy of reaction between the 1,4-semiquinone radical and O_2 of $\Delta H°_r$ = 9.4 kcal/mol, in comparatively poor agreement with the calculated value of 4.5 kcal/mol. Overall, the $\Delta H°_r$ values suggest that the reaction of the 1,2-semiquinone radical with O_2 is 8.1 (experiment-derived) to 13.8 kcal/mol (theoretical) more endothermic than the corresponding reaction of the 1,4-semiquinone radical. It is worth noting that while the theoretical results suggest a difference in $\Delta H°_f$ of 1,2- and 1,4-benzoquinone of roughly 7.9 kcal/mol, in good agreement with Fattahi's difference of 6.7 kcal/mol,[52] the calculated difference in $\Delta H°_f$ of the 1,2- and 1,4-semiquinone of 5.9 kcal/mol is in poor agreement with the estimate derived here from experimental data, which suggest that they are within 1.4 kcal/mol. This is somewhat surprising given that the intramolecular H-bond in the 1,2-semiquinone radicals has recently been estimated from experimental data to be worth 5.6 kcal/mol,[54] a stabilizing interaction absent in 1,4-semiquinone. Given this, and since the $\Delta H°_r$ values for the reaction of the 1,2-semiquinone radical with O_2 are in good agreement, it is tempting to suggest that the value of $\Delta H°_f$ for the 1,4-hydroquinone (measured by Magnus in 1956)[61] may require revision.

The thermochemical data do not aid us in distinguishing which of the two possible mechanisms of the reaction is most likely: direct hydrogen abstraction or the addition−elimination path. However, consideration of the magnitude of the equilibrium constant for hydrogen bonding with the semiquinone radical obtained from our autoxidation studies in the HBA solvents (vide supra, K^S was 1.7 ± 0.7 and 7.8 ± 1.4 M^{-1} for acetonitrile and DMSO, respectively) provides some insight. The α^H_2 values for the H-bond donor species (either the semiquinone radical or the O_2 adduct) we can derive from these K^S by means of Abraham's eq 19[36] are 0.41 and 0.35,

$$\log K^S = 7.354\alpha^H_2\beta^H_2 - 1.094 \quad (19)$$

respectively (see the Supporting Information), and are similar

(54) Lucarini, M.; Pedulli, G. F.; Guerra, M. *Chem. Eur. J.* **2004**, *10*, 933−939.
(55) Mulder, P.; Korth, H.-G.; Pratt, D. A.; DiLabio, G. A.; Valgimigli, L.; Pedulli, G. F.; Ingold, K. U. *J. Phys. Chem. A* **2005**, *109*, 2647−2655.
(56) Benson, S. W. *Thermochemical Kinetics*, 2nd ed.; John Wiley & Sons: New York, 1976.
(57) Ribeiro da Silva, M. D. M. C.; Ribeiro da Silva, M. A. V.; Pilcher, G. *J. Chem. Thermodyn.* **1984**, *16*, 1149−1155.
(58) Lucarini, M.; Pedrielli, P.; Pedulli, G. F.; Cabiddu, S.; Fattuoni, C. *J. Org. Chem.* **1996**, *61*, 9259−9263.
(59) Brigati, G.; Lucarini, M.; Mugnaini, V.; Pedulli, G. F. *J. Org. Chem.* **2002**, *67*, 4828−4832.
(60) The substituent effect of a 4-OH group on the strength of the phenolic O−H bond can be calculated from these data as 86.5 − 81.5 = 5.0 kcal/mol, which is similar to the substituent effect of a 4-OMe group of 88.3 − 82.8 = 5.5 kcal/mol measured previously by some of us using the same REqEPR technique.[59]
(61) Magnus *Physik. Chem.* **1956**, *9*, 141.

SCHEME 9. Origin of the Solvent Effect on the Reactivity of 1,4-Semiquinone Radical with HBA Solvents[a]

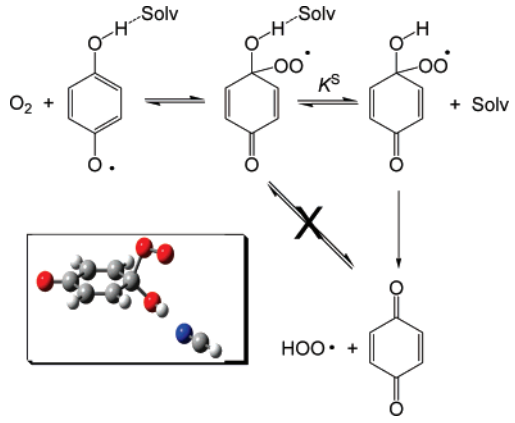

[a] Insert: UB3LYP/6-311G(d,p) model for H-bonding of HCN to the intermediate O_2-adduct.[64]

to values commonly observed for aliphatic alcohols, e.g., methanol $\alpha^H{}_2 = 0.37$.[62] Indeed, if the H-bond donor species interacting with the HBA solvents was the semiquinone radical we would have expected an $\alpha^H{}_2$ value much closer to 1.[63] Thus, the observed solvent effect on the reactivity of 1,4-semiquinone radical with O_2 is probably due to hydrogen bonding of the −OH moiety, which prevents the formation of the intramolecular H-bond that must be formed in order for C−O bond cleavage to occur as in the transition state structure **6D**‡ (Scheme 9).

Conclusions

Hydroquinones are an interesting and important class of chain-breaking antioxidants whose variable behavior is entirely dependent on the fate of the intermediate semiquinone radical, formed upon reaction with chain-carrying peroxyl radicals. The reaction of semiquinone with O_2 to yield hydroperoxyl (superoxide) radicals is the key process sustaining the pro-oxidant activity of hydroquinones and has not been documented for isomeric catechols or analogous phenols. This reaction is believed to be responsible for the ability of the hydroquinone ubiquinol (reduced coenzyme Q_{10}, **IV**) to subvert tocopherol-mediated peroxidation in biological membranes and lipoproteins.[65] It is intimately important in the biological role and function of (hydro)quinones, from the mitochondrial respiratory chain[66] to cytochrome bc_1 complex.[67] We have shown here that it proceeds in nonaqueous media with rate constants (10^6 M^{-1} s^{-1}) comparable to those previously reported in water, but claimed to proceed by a substantially different mechanism.[26] Although such a mechanism has not been documented before,[68,69] the experimental observations and theoretical calculations reported here converge in suggesting that it occurs through a two-step sequence of addition of O_2 to the aromatic ring followed by intramolecular H-atom transfer concerted with cleavage of the hydroperoxyl moiety.

Experimental Section

Materials. Solvents were of the highest grade commercially available and were used as received. α,α′-Azobis(isobutyronitrile), AIBN, was stored at −20 °C and used without further purification; 2,2′-azobis(2,4-dimethylvaleronitrile), AMVN, was available from previous studies and was purified by crystallization from hexane. *RRR*-α-Tocopherol was purified by column chromatography on silica gel eluting with 92:8 hexane/ethyl acetate as previously described.[37c] Styrene (99+%) was distilled under reduced pressure and purified by percolation through silica (twice) and through activated basic alumina (once). Di-*tert*-butyl peroxide was similarly purified by percolation. 2,5-Di-*tert*-butylhydroquinone, 2,5-di-*tert*-amylhydroquinone, and 2,6-di-*tert*-butyl-4-methylphenol (BHT) were commercially available and used without further purification.

Laser Flash Photolysis. The laser flash photolysis equipment and experimental procedures have been adequately described in earlier publications.[28] Experiments were carried out at 298 ± 2 K in cells made of 7 × 7 mm^2 Suprasil quartz tubing. Solutions (in chlorobenzene or acetonitrile) were either equilibrated with air or sealed with a rubber septum and bubbled with oxygen. *tert*-Butoxyl radicals were generated by 308 nm LFP (excimer laser, XeCl gas mixture) of solutions of di-*tert*-butyl peroxide (0.15−0.30 M) in the presence of 2,5-di-*tert*-butylhydroquinone (QH_2). The peroxide concentrations were chosen so as to give an OD of ∼0.3 at the laser wavelength. UV spectra of the transients were collected 0.8−3 μs after the laser pulse. The time-evolution of the transient species was monitored at 420 nm. Digitally averaged decay curves from five to ten laser flashes were collected. The QH_2 concentrations (0.1−2 mM) were chosen to obtain transient lifetimes of 5−50 μs, and to avoid excessive absorbance at the laser wavelength. Decay traces were first roughly reproduced by stochastic simulation using CKS 1.0 software, developed at IBM (Almaden, San Jose, CA), then the best kinetic constants used in simulations were optimized by interactive numerical fitting to the 10−12 experimental traces for each solvent using Gepasi software, version 3.30,[29] and the reaction scheme represented by eqs 9−13 (see the Supporting Information).

Inhibited Autoxidations. Autoxidation experiments were performed in a two-channel oxygen uptake apparatus, based on a Validyne DP 15 differential pressure transducer, described elsewhere.[31] The entire apparatus was immersed in a thermostated bath ensuring a constant temperature within ±0.1 °C. In a typical experiment, an air-saturated solution of styrene (4.3 M) containing either AMVN (5×10^{-3} M) or AIBN (5×10^{-2} M) was equilibrated with a reference solution containing an excess of α-tocopherol (1×10^{-4} M) at 30 °C. When a constant oxygen consumption rate was reached, a small amount of a chlorobenzene

(62) Abraham, M. H.; Grellier, P. L.; Prior, D. V.; Duce, P. P.; Morris, J. J.; Taylor, P. J. *J. Chem. Soc., Perkin Trans. II* **1989**, 699−711.

(63) Phenol has $\alpha_H{}^2 = 0.596$ and this value increases with electron-withdrawing substituents in the 4-position on the aromatic ring, e.g., 4-fluorophenol ($\alpha_H{}^2 = 0.629$), 4-cyanophenol ($\alpha_H{}^2 = 0.772$), 4-nitrophenol ($\alpha_H{}^2 = 0.824$).[62]

(64) The calculated solvent effect on the elimination of HOO• is 3.3 kcal/mol. While this is larger than the observed effect on the rate constant (roughly one order of magnitude), it should be noted that in our calculations we are comparing the isolated O_2-adduct in the gas phase with the O_2-adduct H-bonded to HCN in the gas phase. It is totally reasonable that this would be overestimated relative to the O_2 adduct H-bonded to chlorobenzene compared to the O_2-adduct H-bonded to acetonitrile in our experiments.

(65) Bowry, V. W.; Ingold, K. U. *Acc. Chem. Res.* **1999**, *32*, 27−34.

(66) Schultz, B. E.; Chan, S. I. *Annu. Rev. Biophys. Biomol. Struct.* **2001**, *30*, 23−65.

(67) (a) Cape, J. L.; Bowman, M. K.; Kramer, D. M. *J. Am. Chem. Soc.* **2005**, *127*, 4208−4215. (b) Yap, L. L.; Samoilova, R. I.; Gennis, R. B.; Dikanov, S. A. *J. Biol. Chem.* **2006**, *281*, 16879−16887.

(68) After this manuscript was completed we become aware that a kinetic investigation on the reaction of anthrasemiquinone radical with oxygen in nonaqueous media had been previously performed by A. S. Tatikolov.[69] In that work the solvent effect was studied in some detail. When processed with the Abraham equation (eq 19), those kinetic data afford $\alpha_H{}^2 = 0.37$ for the reaction intermediate, in excellent agreement with the values obtained in the present work. In that paper a somewhat similar reaction mechanism was also tentatively suggested, i.e., a cyclic transition state with the oxygen complexed to the π system of the aromatic ring. We thank Dr. Peter Mulder for pointing out this reference.

(69) Tatikolov, A. S. *Russ. Chem. Bull.* **1997**, *46*, 1082−1087.

solution of the antioxidant was added to the autoxidating mixture and the oxygen consumption in the sample was measured from the differential pressure between the two channels recorded as a function of time. This instrumental setting allowed us to have the N_2 production and the oxygen consumption derived from the azoinitiator decomposition already subtracted from the measured reaction rates. Induction period lengths (τ) were determined by the intersection between the regression lines to the inhibited and the uninhibited traces. Initiation rates, R_i, were determined in preliminary experiments by the inhibitor method, using α-tocopherol as reference antioxidant: $R_i = 2[\alpha\text{-TOH}]/\tau$.[43]

Experiments were performed with either 2,5-di-*tert*-butylhydroquinone (0.6×10^{-5} to 6×10^{-5} M) or its structural analogue 2,5-di-*tert*-amylhydroquinone, which was sometimes preferred due to the higher solubility in chlorobenzene. The co-antioxidant behavior of 2,5-di-*tert*-butylhydroquinone (QH_2) was investigated by using 1:1 and 1:2 antioxidant mixtures of QH_2 (5×10^{-6} M) and α-tocopherol. Numerical simulation of oxygen consumption traces was performed by using Gepasi software, version 3.30.[29]

EPR and Thermochemical Measurements. Deoxygenated isooctane solutions containing 2,5-di-*tert*-amylhydroquinone (0.01−0.001 M) and BHT (0.01−0.001 M) in variable ratios were sealed under nitrogen in a Suprasil quartz EPR tube. The sample was inserted at room temperature in the cavity of a Bruker ESP 300 EPR spectrometer and photolyzed with the unfiltered light from a 500 W high-pressure mercury lamp. The temperature was controlled with a standard variable temperature accessory and was monitored before and after each run with a copper−constantan thermocouple. Spectra were recorded a few seconds after starting to irradiate to avoid significant consumption of the phenols during the course of the experiment, with the following instrumental settings: microwave frequency 9.74 GHz, power 6.4 mW, modulation amplitude 0.1−0.5 G, center field 3320 G. The following spectral parameters were observed for the equilibrating radical species: $QH^{\bullet}$, $a_H = 5.31$ G (1H, ortho), 1.01 G (1H, meta), 1.32 G (1H, *OH*), $g = 2.0048$; $BHT^{\bullet}$, $a_H = 1.74$ G (2H, meta), 11.15 G (3H, CH_3), $g = 2.0046$. Relative radical concentrations were determined by comparison of the digitized experimental spectra with computer simulated ones, as previously described.[58]

Theoretical Calculations. The calculations described in this paper were originally performed with the complete basis set-quadratic Becke3 (CBS-QB3) model of Petersson and co-workers.[70] This model chemistry attempts to estimate the CCSD(T)/CBS energy by using an extrapolation scheme based on UMP2 wave functions. We have found that in some of the cases studied here, the UMP2 step—and hence the extrapolation to the CBS limit—led to spurious results, presumably due to the significant spin contamination in the unrestricted wave functions. In the spirit of a recent report by Petersson and co-workers,[71] we used the UB3LYP/6-311G(d,p) optimized geometries from our CBS-QB3 calculations and estimated the CCSD(T)/CBS energy based on MP2 calculations carried out with restricted open shell wave functions (ROMP2). The estimate is based on a two-point extrapolation[72] of the CCSDT/aug-cc-pVDZ energy using ROMP2 electronic energies determined with the aug-cc-pVDZ and aug-cc-pVTZ basis sets. These electronic energies were then combined with zero-point vibrational energies and thermochemical corrections obtained at the UB3LYP/6-311G(d,p) level to obtain the energies and thermochemical quantities reported herein. All calculations were performed with the Gaussian 03 suite of programs[73] and all of the relevant geometries, energies, and thermochemical corrections are provided as Supporting Information.

Acknowledgment. We acknowledge thoughtful discussion with Dr. Peter Mulder. This work was supported by grants to L.V., G.F.P., and R.A. from the University of Bologna and MIUR (Rome) and to D.A.P. from the Natural Science and Engineering Research Council of Canada and the Canada Research Chairs program. This research has been enabled by the use of HPCVL and WestGrid computing resources, funded in part by the Canada Foundation for Innovation, the Ontario Innovation Trust, Alberta Innovation and Science, BC Advanced Education, and the participating research institutions. G.A.D. also thanks the Centre for Excellence in Integrated Nanotools (University of Alberta) for access to additional computing facilities. L.V., G.F.P., and R.A. thank Prof. Marco Lucarini for access to the EPR simulation software in REqEPR experiments.

Supporting Information Available: Cartesian coordinates and relevant energies for all calculated structures reported herein, details of the numerical fitting of the laser flash photolysis and inhibited autoxidation data, and details of the determination of the solvent binding constants. This material is available free of charge via the Internet at http://pubs.acs.org.

JO7024543

(70) (a) Montgomery, J. A., Jr.; Frisch, M. J.; Ochterski, J. W.; Petersson, G. A. *J. Chem. Phys.* **1999**, *110*, 2822−2827. (b) Montgomery, J. A., Jr.; Frisch, M. J.; Ochterski, J. W.; Petersson, G. A. *J. Chem. Phys.* **2000**, *112*, 6532−6542.

(71) Wood, G. P. F.; Radom, L.; Petersson, G. A.; Barnes, E. C.; Frisch, M. J.; Montgomery, J. A., Jr. *J. Chem. Phys.* **2006**, *125*, 94106−94116.

(72) Martin, J. M. L. *Chem. Phys. Lett.* **1996**, *259*, 669−678.

(73) Frisch, M. J.; Trucks, G. W.; Schlegel, H. B.; Scuseria, G. E.; Robb, M. A.; Cheeseman, J. R.; Montgomery, J. A., Jr.; Vreven, T.; Kudin, K. N.; Burant, J. C.; Millam, J. M.; Iyengar, S. S.; Tomasi, J.; Barone, V.; Mennucci, B.; Cossi, M.; Scalmani, G.; Rega, N.; Petersson, G. A.; Nakatsuji, H.; Hada, M.; Ehara, M.; Toyota, K.; Fukuda, R.; Hasegawa, J.; Ishida, M.; Nakajima, T.; Honda, Y.; Kitao, O.; Nakai, H.; Klene, M.; Li, X.; Knox, J. E.; Hratchian, H. P.; Cross, J. B.; Bakken, V.; Adamo, C.; Jaramillo, J.; Gomperts, R.; Stratmann, R. E.; Yazyev, O.; Austin, A. J.; Cammi, R.; Pomelli, C.; Ochterski, J. W.; Ayala, P. Y.; Morokuma, K.; Voth, G. A.; Salvador, P.; Dannenberg, J. J.; Zakrzewski, V. G.; Dapprich, S.; Daniels, A. D.; Strain, M. C.; Farkas, O.; Malick, D. K.; Rabuck, A. D.; Raghavachari, K.; Foresman, J. B.; Ortiz, J. V.; Cui, Q.; Baboul, A. G.; Clifford, S.; Cioslowski, J.; Stefanov, B. B.; Liu, G.; Liashenko, A.; Piskorz, P.; Komaromi, I.; Martin, R. L.; Fox, D. J.; Keith, T.; Al-Laham, M. A.; Peng, C. Y.; Nanayakkara, A.; Challacombe, M.; Gill, P. M. W.; Johnson, B.; Chen, W.; Wong, M. W.; Gonzalez, C.; Pople, J. A. *Gaussian 03*, Revision C.02; Gaussian, Inc.: Wallingford, CT, 2004.